

Supplement of

Top–down estimates of black carbon emissions at high latitudes using an atmospheric transport model and a Bayesian inversion framework

Nikolaos Evangeliou et al.

* Correspondence to: N. Evangeliou (nikolaos.evangeliou@nilu.no)

COMPARISON OF PRIOR SIMULATED CONCENTRATIONS (ACCMIPv5) (YEARS 2013-2015)

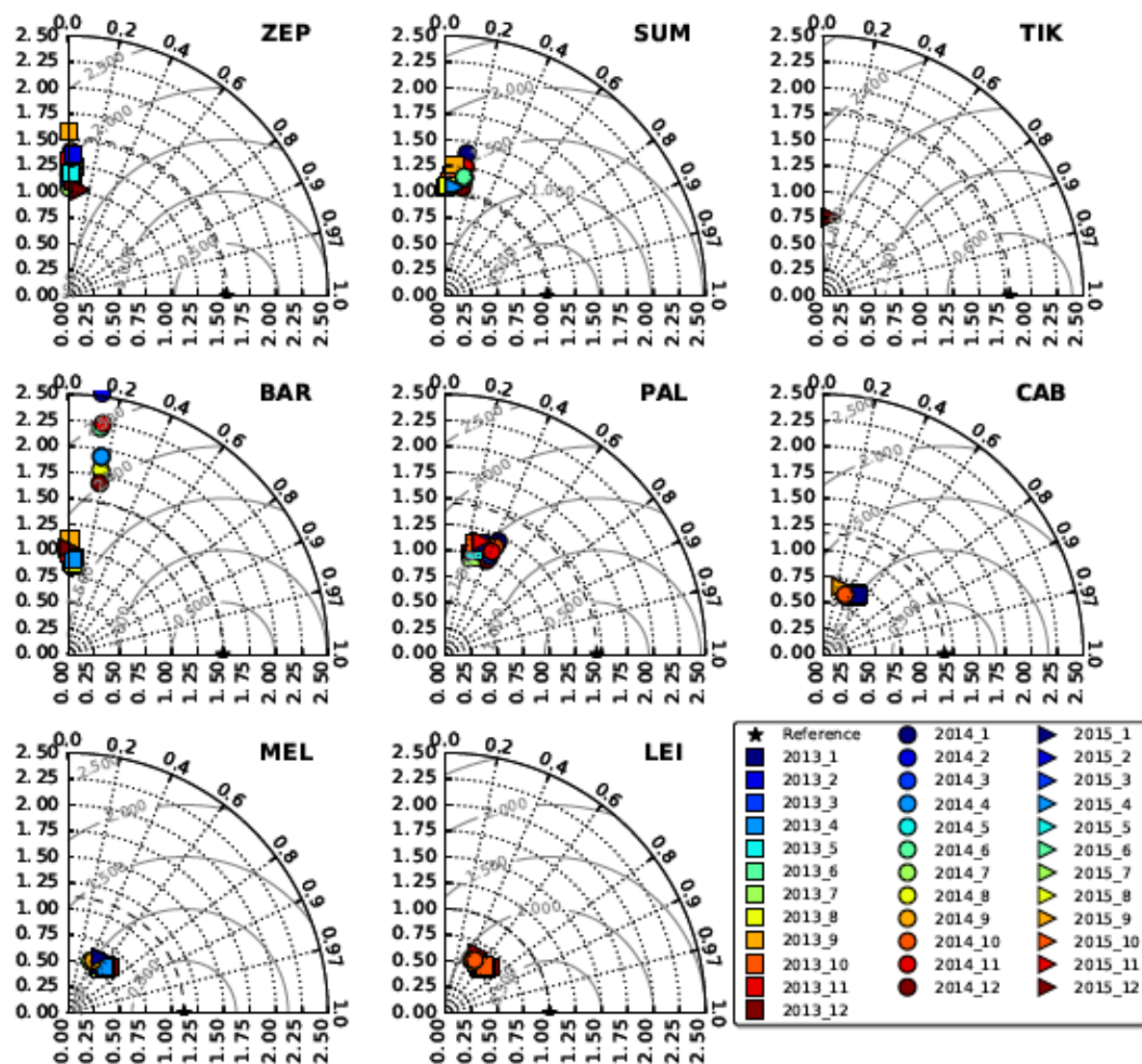


Figure S 1. Taylor diagrams for the comparison of the prior simulated concentrations with observations for all years (2013 – 2015) for 12 BC species with different scavenging coefficients (Table 2). The radius indicates standard deviations normalised against the mean concentration (NSD); the azimuthal angle the Pearson correlation coefficient, while the normalised (against observation) root mean square error (nRMSE) in the simulated concentrations is proportional to the distance from the point on the x-axis identified as “reference” (grey contours). The results refer to the use of ACCMIPv5, EDGAR-HTAPv2.2 and MACCcity as the prior emissions.

**COMPARISON OF PRIOR SIMULATED CONCENTRATIONS (EDGAR_HTAPv2.2)
(YEARS 2013-2015)**

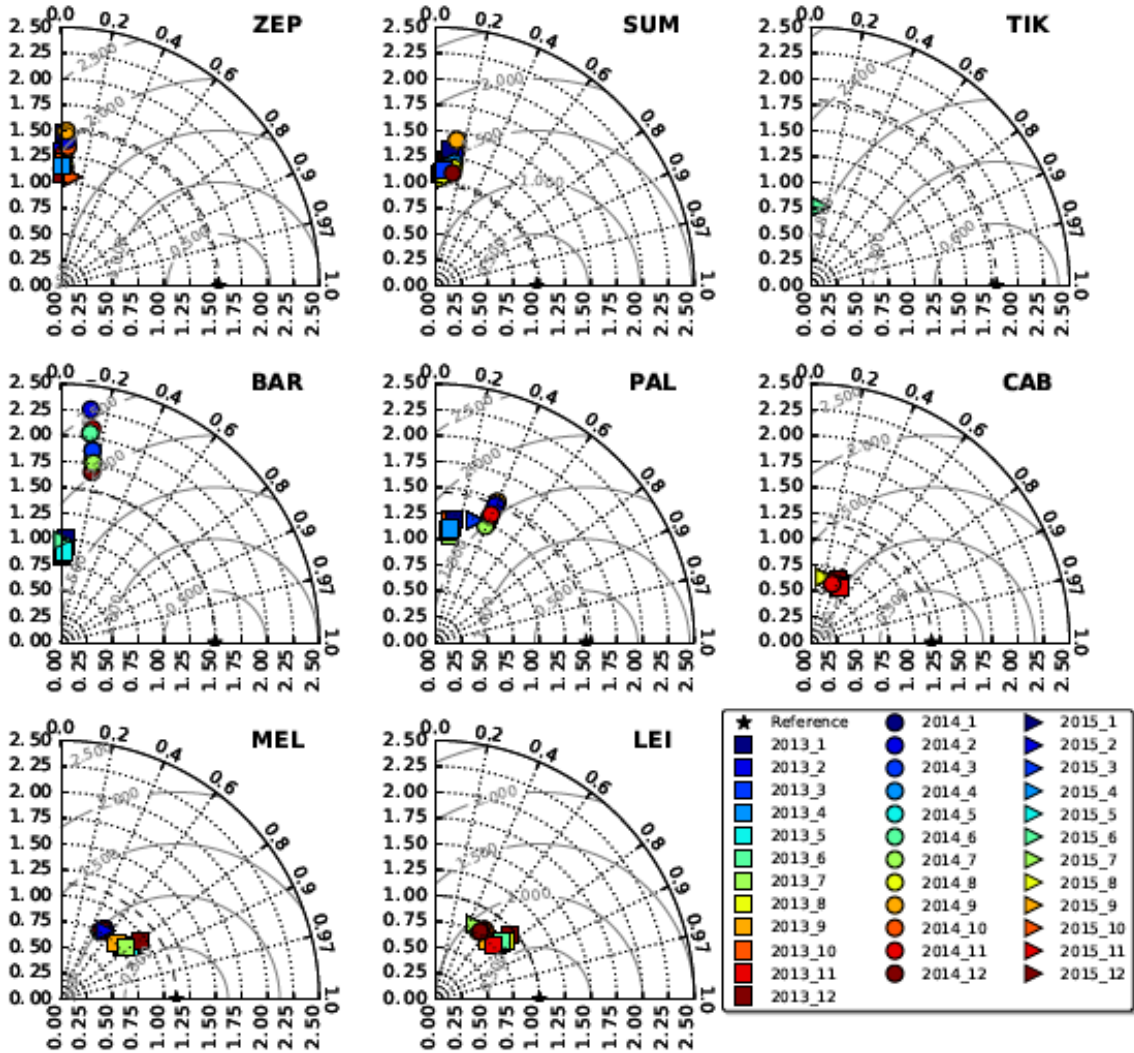


Figure S 1. Continued

**COMPARISON OF PRIOR SIMULATED CONCENTRATIONS (MACCITY)
(YEARS 2013-2015)**

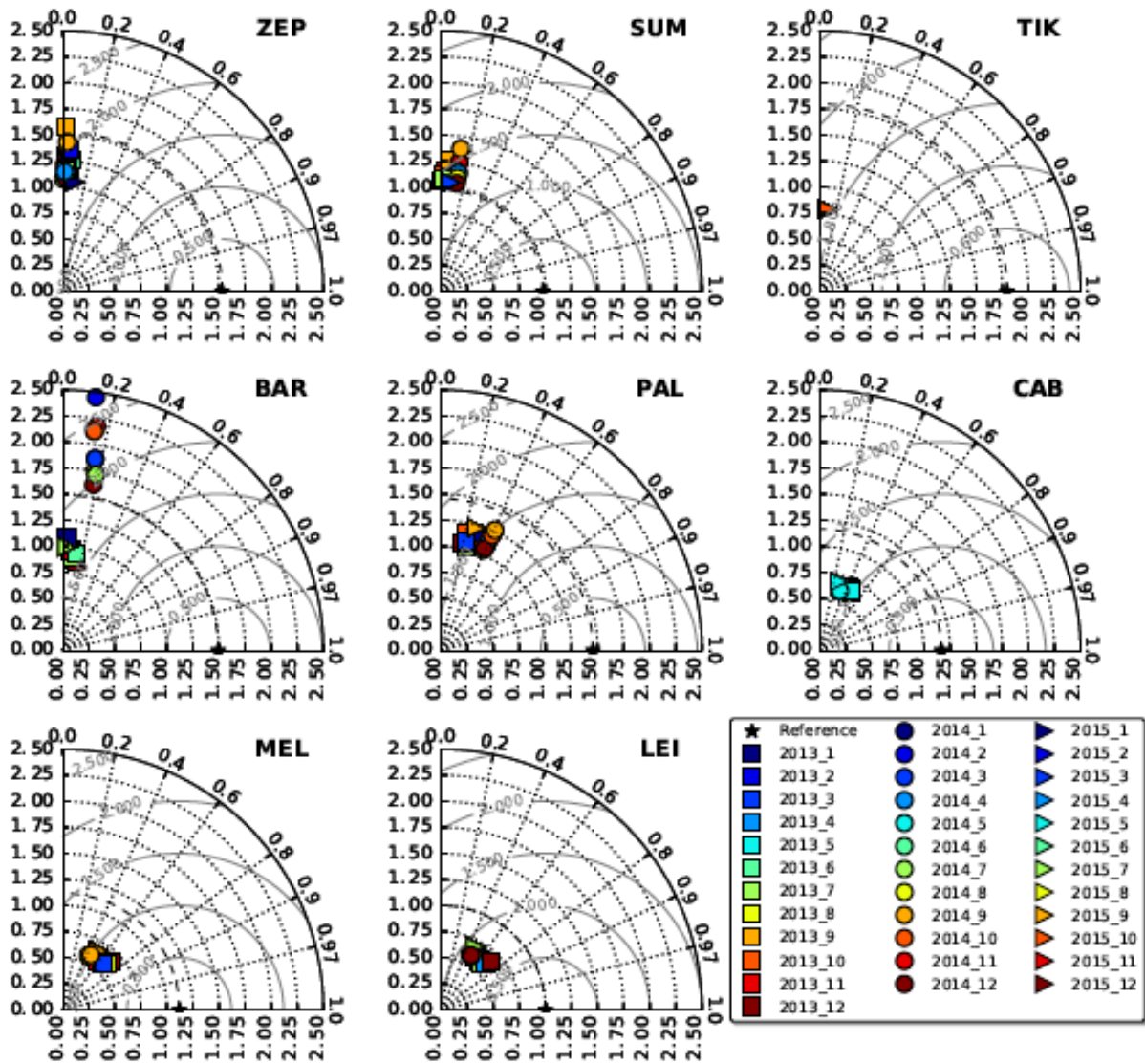


Figure S 1. Continued

**MONTHLY AVERAGE MODEL-OBSERVATION MISMATCHES
FOR 12 BC SPECIES (2013)**

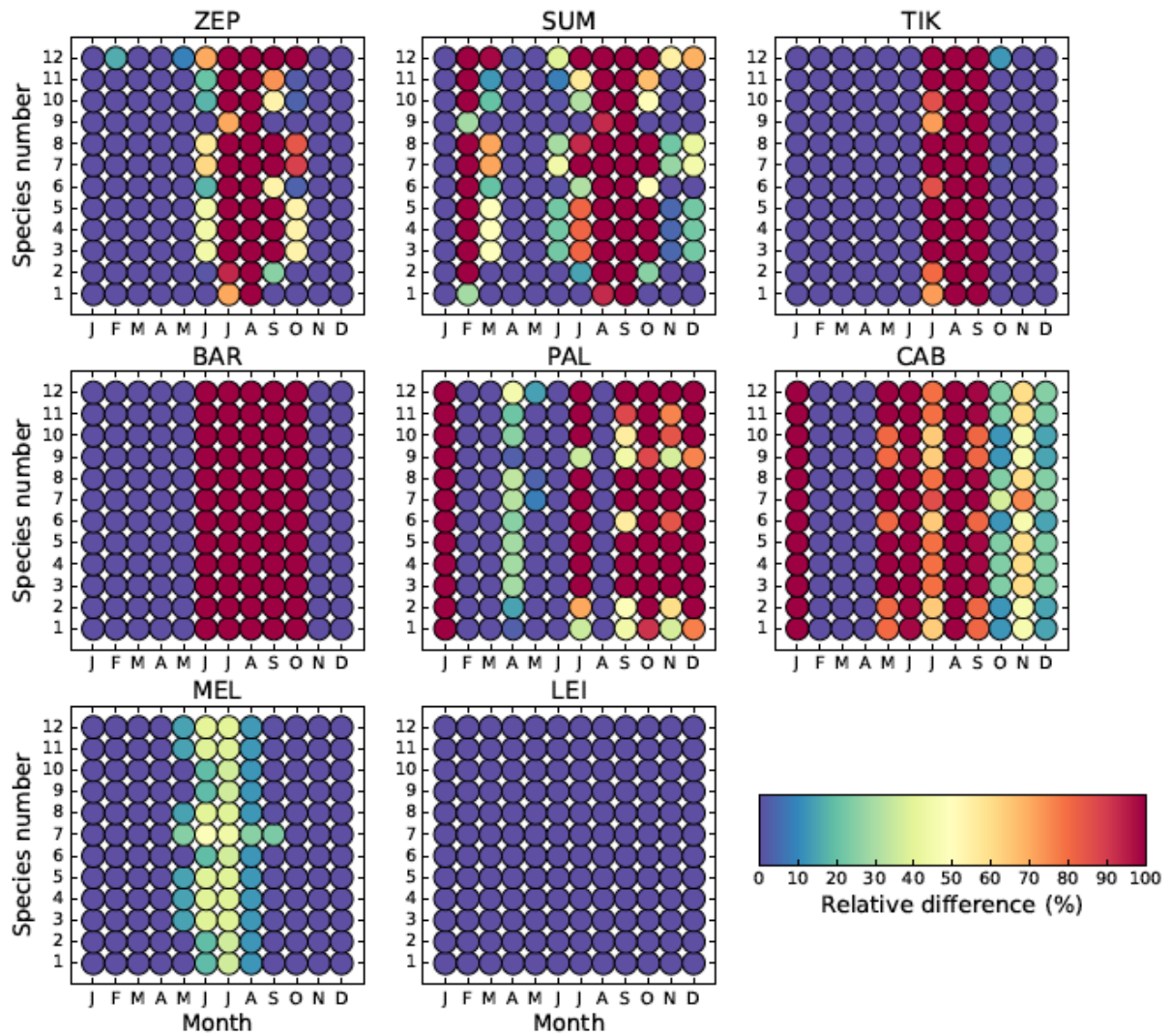


Figure S 2. Monthly average relative model-observation mismatches ($[\text{model} - \text{observations}]/\text{observations}$) for prior simulated (average values from all four inventories used) concentrations of BC due to the perturbation of scavenging parameters according to Table 2 for the inversions of 2013, 2014 and 2015.

**MONTHLY AVERAGE MODEL-OBSERVATION MISMATCHES
FOR 12 BC SPECIES (2014)**

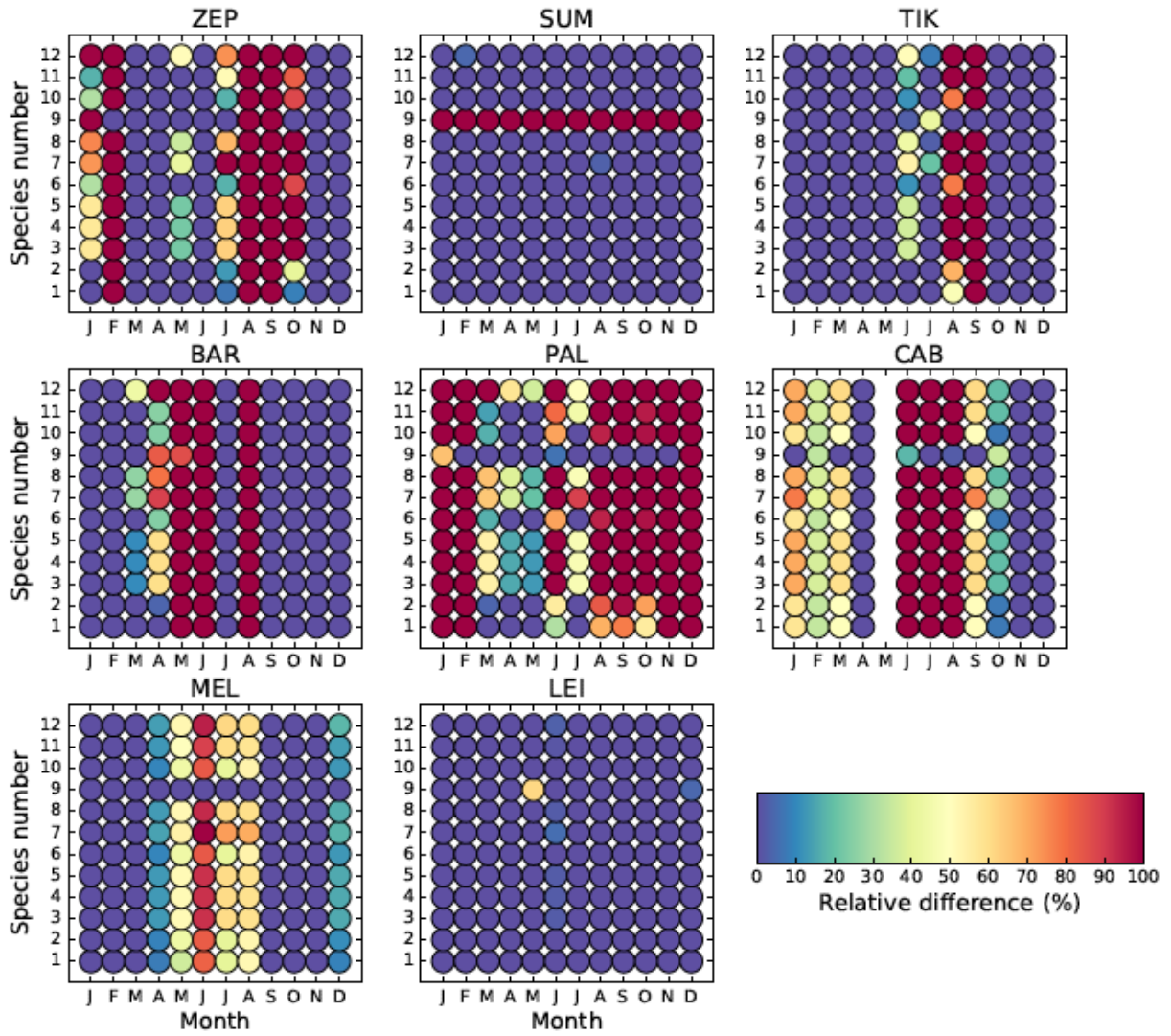


Figure S 2. Continued

**MONTHLY AVERAGE MODEL-OBSERVATION MISMATCHES
FOR 12 BC SPECIES (2015)**

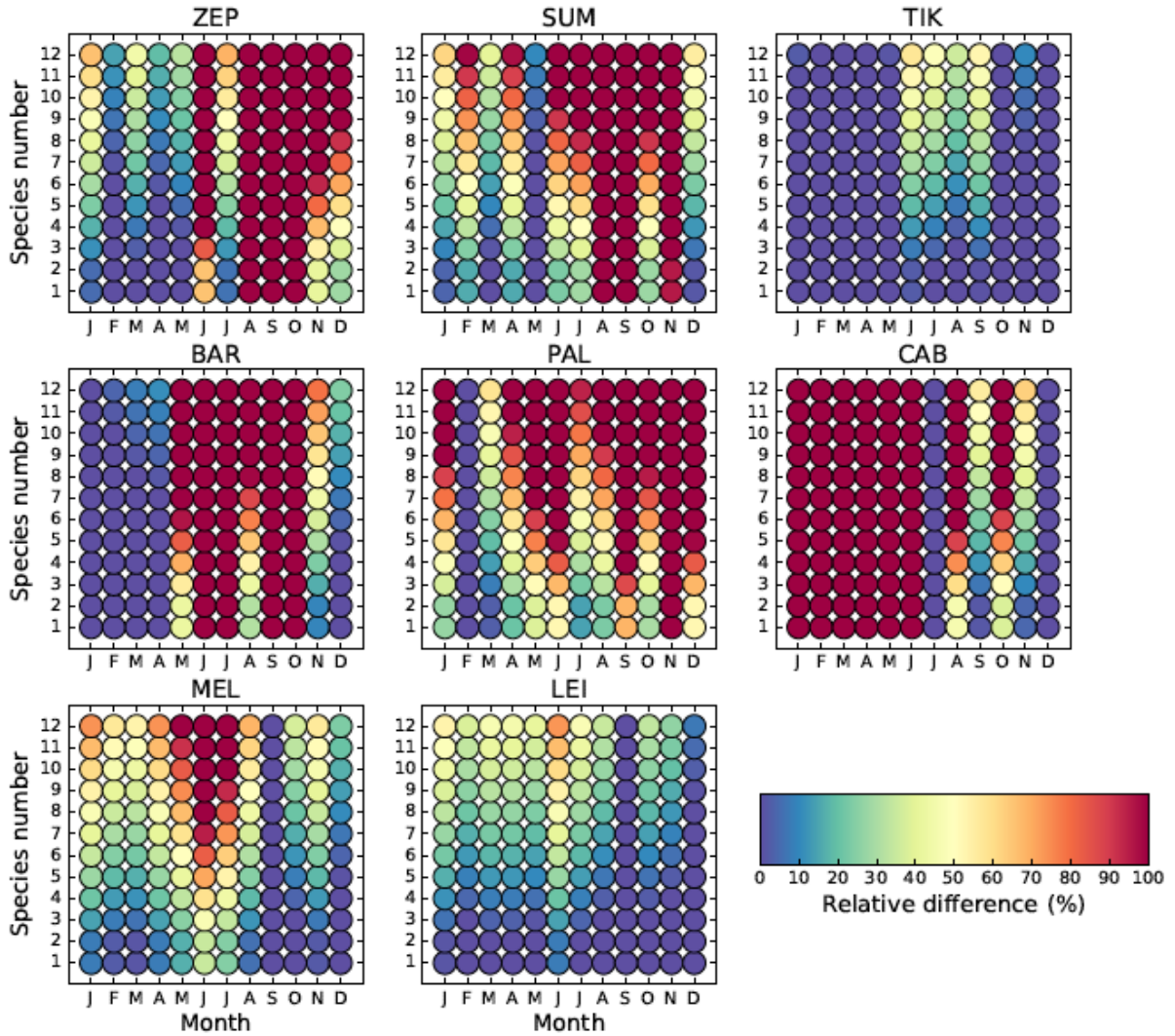


Figure S 2. Continued.

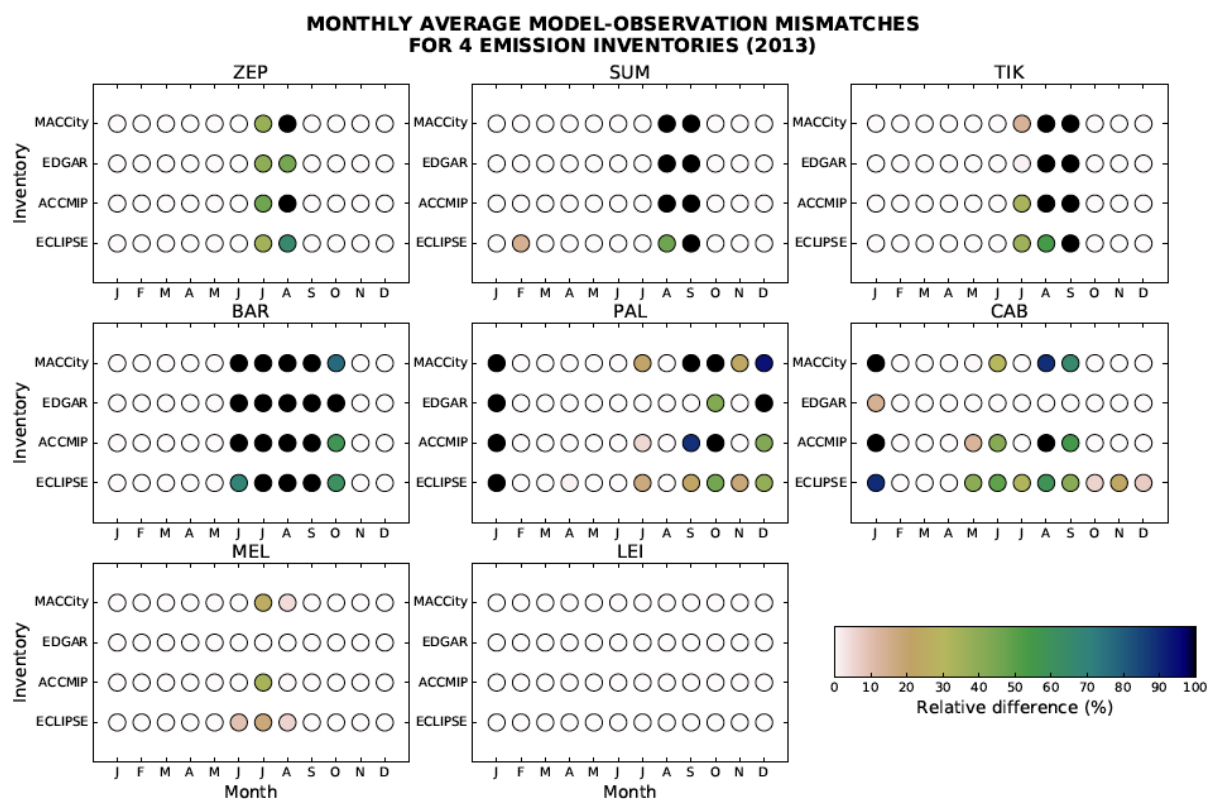


Figure S 3. Monthly average model-observation mismatches ($[\text{model} - \text{observations}] / \text{observations}$) for prior simulated concentrations of BC (best species) due to use for four different emission inventories (ECLIPSEv5, ACCMIPv5, EDGAR_HTAPv2.2 and MACCity) for the inversions of 2013, 2014 and 2015.

**MONTHLY AVERAGE MODEL-OBSERVATION MISMATCHES
FOR 4 EMISSION INVENTORIES (2014)**

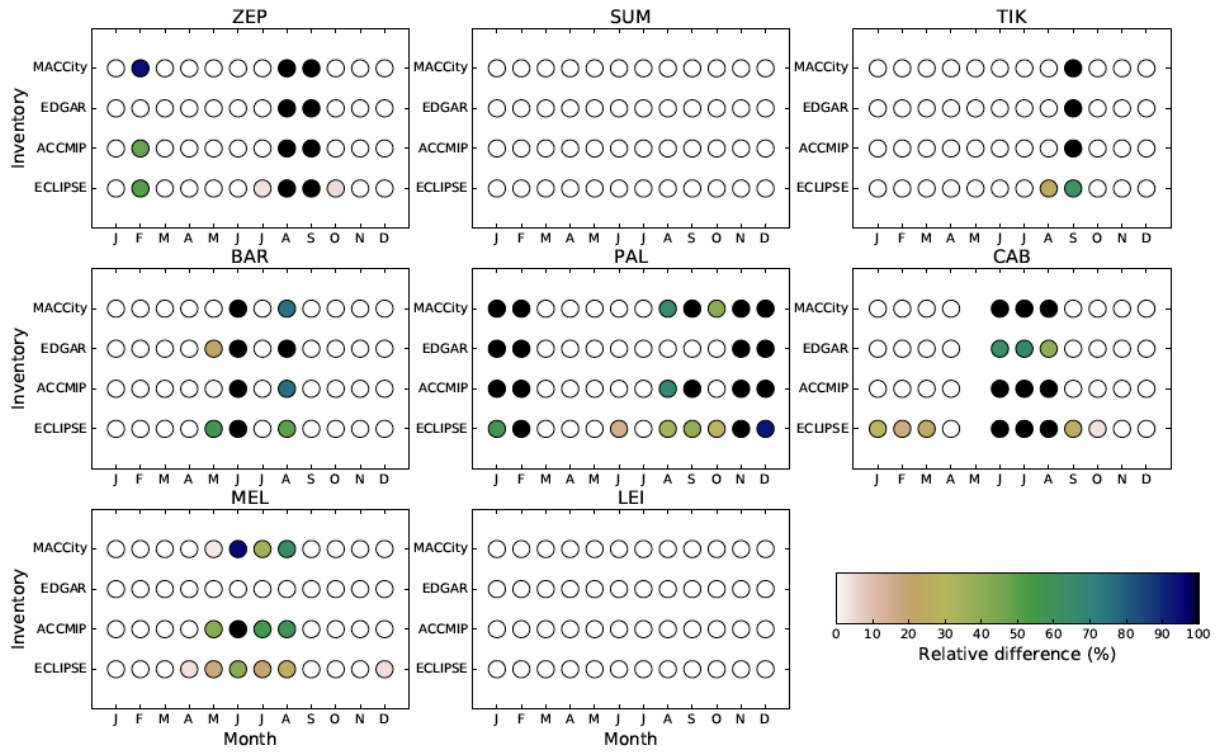


Figure S 3. Continued.

**MONTHLY AVERAGE MODEL-OBSERVATION MISMATCHES
FOR 4 EMISSION INVENTORIES (2015)**

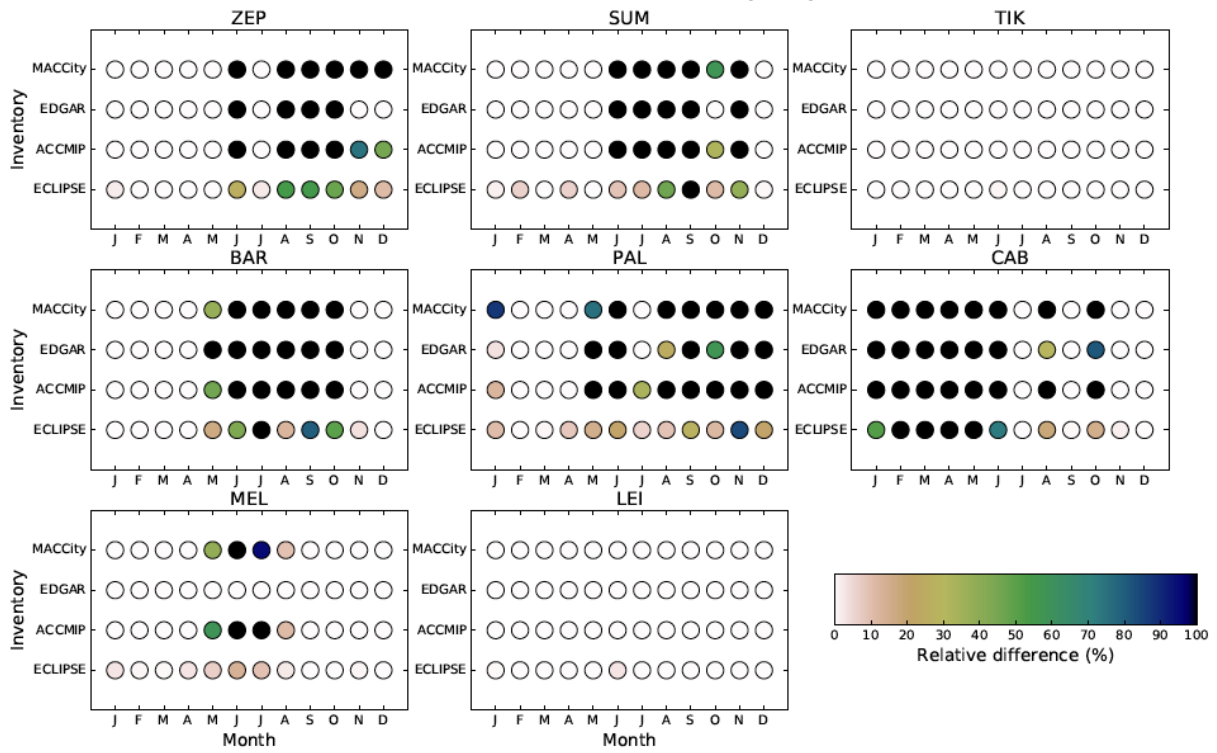


Figure S 3. Continued.

COMPARISON OF POSTERIOR SIMULATED CONCENTRATIONS (YEARS 2013-2015)

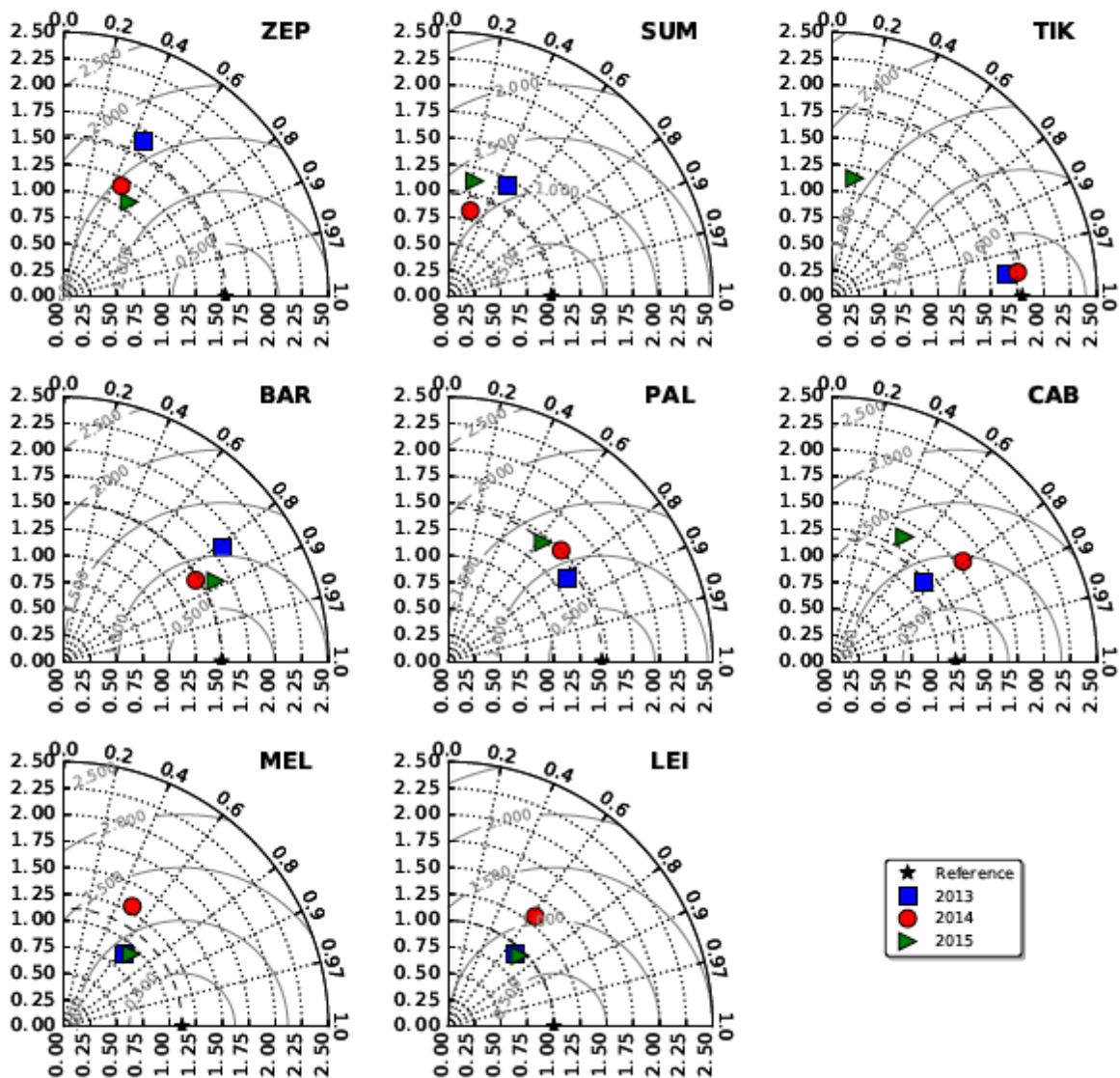


Figure S 4. Taylor diagrams for the comparison of the posterior simulated concentrations with observations for all years (2013 – 2015). The radius indicates standard deviations normalised against the mean concentration (NSD); the azimuthal angle the Pearson correlation coefficient, while the normalised (against observation) root mean square error (nRMSE) in the simulated concentrations is proportional to the distance from the point on the x-axis identified as “observed” (grey contours).

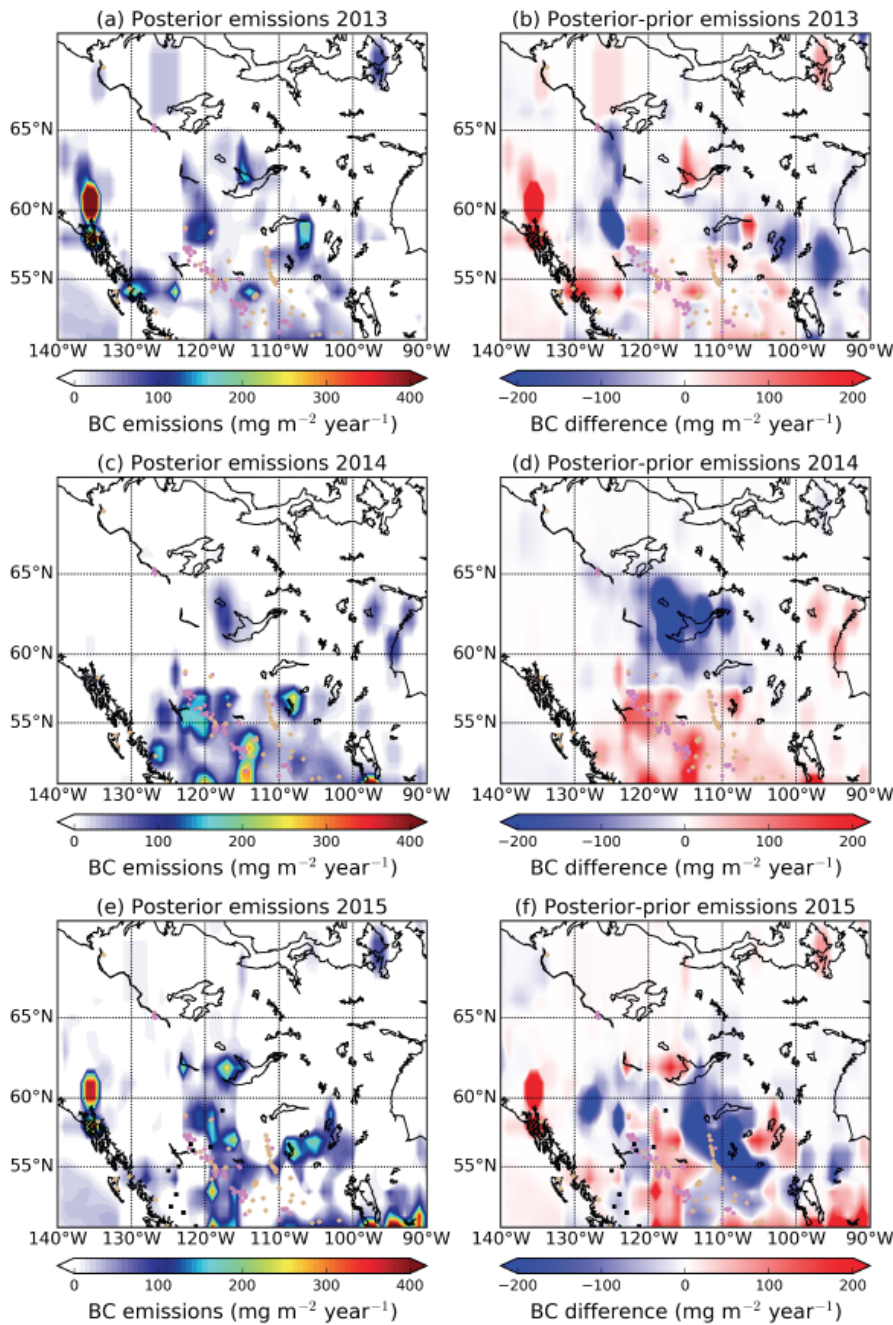


Figure S 5. (a, c, e) Optimised emissions of BC in North America (Western Canada) for 2013, 2014 and 2015. (b, d, f) Difference between a posteriori and a priori emissions of BC (ECLIPSEv5 was used as the prior). Magenta points on the map denote the gas flaring industries from the Global Gas Flaring Reduction Partnership (GGFR) (<http://www.worldbank.org/en/programs/gasflaringreduction>), grey points show the power industries that operate using fossil fuels and oil and gas production and oil refining industries adopted from Industry About (<https://www.industryabout.com/canada-industrial-map>), while black rectangles show active fires from MODIS.

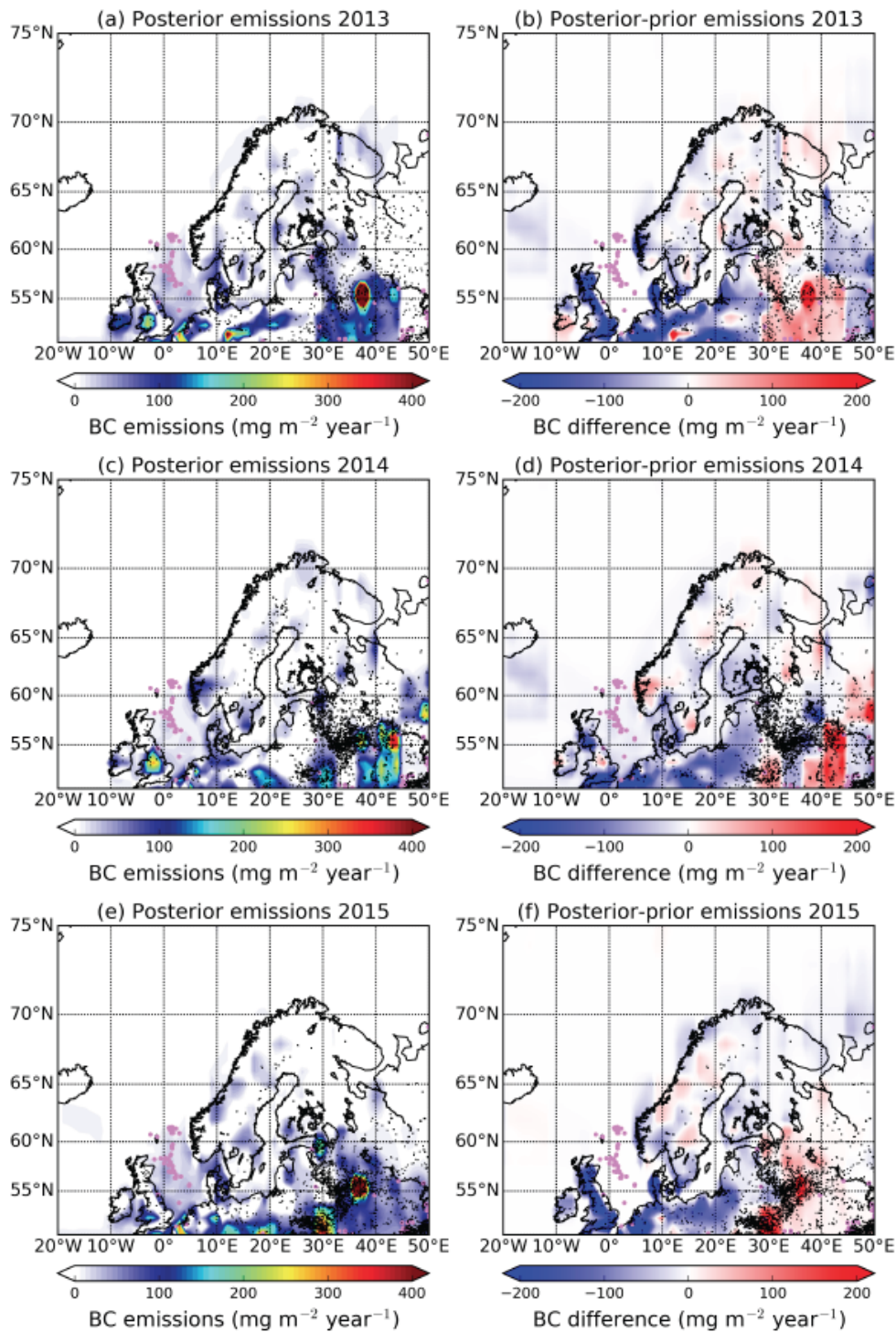


Figure S 6. (a, c, e) Optimised emissions of BC in Northern Europe for 2013, 2014 and 2015. (b, d, f) Difference between a posteriori and a priori emissions of BC (ECLIPSEv5 was used as the prior). Magenta points on the map indicate the gas flaring industries from the Global Gas Flaring Reduction Partnership (GGFR) (<http://www.worldbank.org/en/programs/gasflaringreduction>), while black rectangles show vegetation fires adopted from Hao et al. (2016).

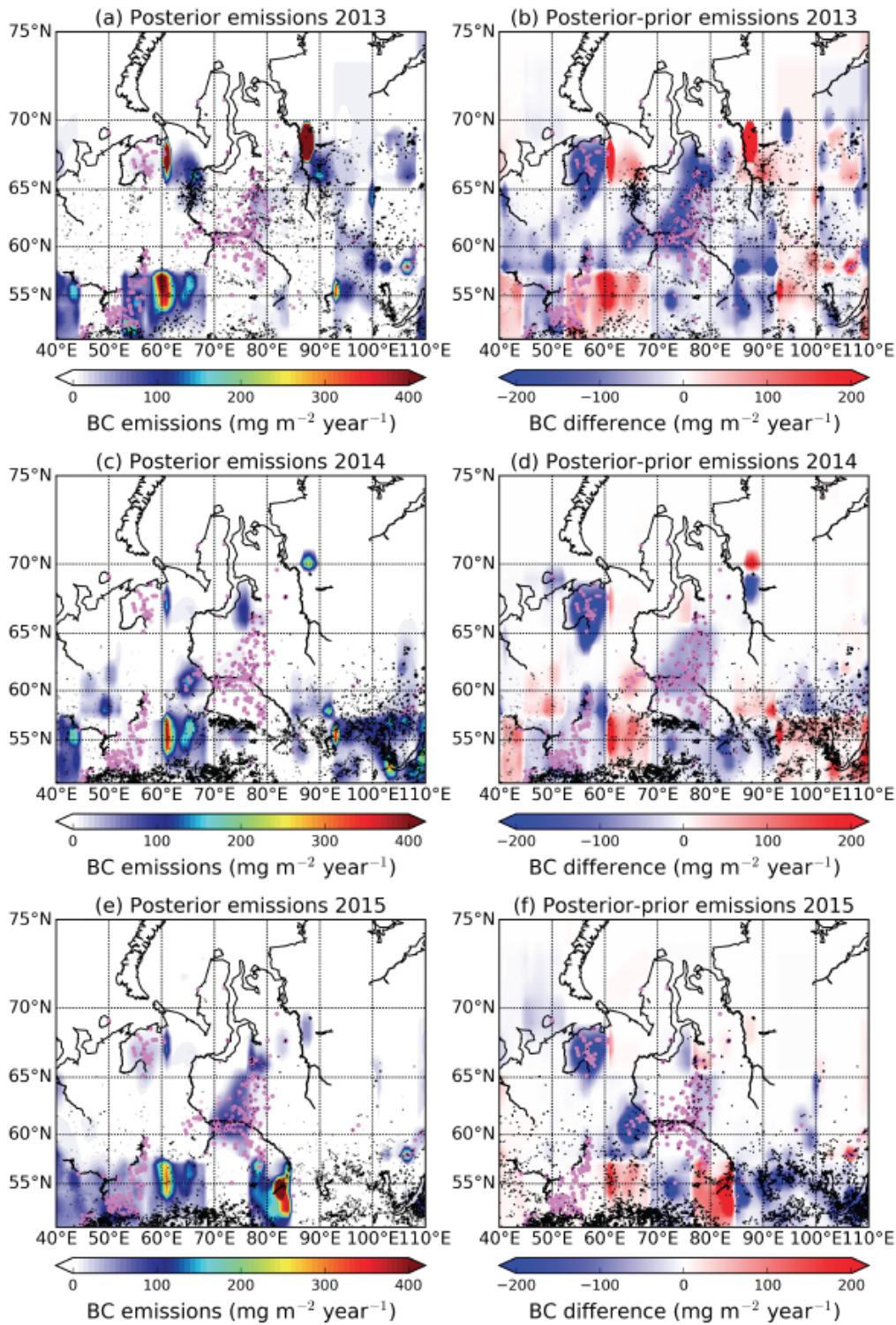


Figure S 7. (a, c, e) Optimised emissions of BC in Western Siberia for 2013, 2014 and 2015. (b, d, f) Difference between a posteriori and a priori emissions of BC (ECLIPSEv5 was used as the prior). Magenta points on the map indicate the gas flaring industries from the Global Gas Flaring Reduction Partnership (GGFR) (<http://www.worldbank.org/en/programs/gasflaringreduction>), while black rectangles show forest fires adopted from Hao et al. (2016).